

# Morphology control of clay-mineral particles as supports for metallocene catalysts in propylene polymerization

Takao Tayano<sup>\*1</sup>, Takehiro Sagae<sup>1</sup>, Takashi Atsumi<sup>1</sup>, Hideshi Uchino<sup>1</sup>, Masahide Murata<sup>1</sup>, Tsutomu Sato<sup>2</sup>

<sup>1</sup> Research and Development Division, Japan Polychem Corporation, 1, Toho-cho Yokkaichi, Mie 510-0848, Japan

<sup>2</sup> Graduate school of Engineering, Hokkaido University, Kita 13, Nishi 8, Kita-ku, Sapporo, 060-8628, Japan

Received: 28 July 2015, Accepted: 14 October 2015

---

## ABSTRACT

Spray-dry granulation of clay minerals was studied to obtain clay mineral base support material for metallocene supported olefin polymerization catalysts. The morphology of the granules was strongly influenced by the nature of the clay mineral itself. Because of swelling characteristics of montmorillonite, its water dispersion was highly viscous even in the low slurry concentration (< 4 wt %). Therefore, it was very difficult to control the granule characteristics such as size, shape, and inside structure by the spray drying of the clay mineral slurry. Then we examined some methods in order to change the clay mineral surface properties for getting less viscous dispersion. It was found that the milling of montmorillonite increased the amount of surface OH groups. This surface characteristic change should promote the interaction between the edges and basal planes of the primary particles of milled montmorillonite, resulting in the lowering the slurry viscosity. The milling is effective for overcoming difficulty in use of high concentration montmorillonite slurry in spray-dry granulation which is indispensable for producing granules in the wide range of size (10–50 μm). The spray-dried montmorillonite granules are useful as a "support-activator" for an olefin polymerization catalyst combined with metallocenes. **Polyolefins J (2016) 3: 79-92**

**Keywords:** metallocene catalyst; activator; clay minerals; support; spray-dry

---

## INTRODUCTION

The polypropylene production process is very different from the others for liquid or gaseous chemicals. The raw material, liquid or gaseous propylene, is supplied into a reactor and converted into solid polypropylene particles, which are then transferred to an extruder through several pipes on a stream of carrier gas. If the product particles have poor fluidity, serious operational issues, such as line plugging may happen. The physical properties of polymer particles are a key concern to achieve stable plant operations.

Meanwhile, it is well known that there is a "replica" relationship between catalyst and polymer particles [1, 2]. During polymerization, polymer particles can grow as replicas of the catalyst particles so that the catalyst particles are broken up into sub-particles and dispersed in the polymer phase. Therefore, polymer particle morphology is generally controlled through design of the catalyst particle morphology, such as shape, size, and strength. Spherical polymer particles are required for smooth movement in the process. Catalyst particles having a size of 10–60 μm are commonly used, and the most suitable particle size is chosen to complement

---

\* Corresponding Author - E-mail: Tayano.Takao@mp.pochem.co.jp

the characteristics of the polymerization process. For example, a smaller catalyst is suitable for the propylene bulk process, whereas a larger one is used for the gas-phase process. Furthermore, it is important for the catalyst particles to have appropriate strength. For instance, they should be weak enough to allow polymer particle growth during the polymerization process, but strong enough to avoid generating fines in the reactor and the polymer powder transfer lines.

Numerous efforts have been devoted to creating catalyst particles having the desired shape, size, and strength [3, 4]. Crystalline polypropylene has been produced by heterogeneous catalysts [5]. Using conventional Ziegler–Natta catalysts, excellent catalyst particle control was accomplished for both Solvay type catalysts [6] and  $MgCl_2$  supported catalysts [7].

Recently, metallocene based new generation catalysts have been attracting much attention in the field of olefin polymerization because such catalysts are more suitable for the precise design of polymer structures than conventional catalysts [8, 9, 10]. The basic catalyst system comprises a metallocene complex and a soluble co-catalyst, such as MAO, borane, or borate [11, 12], thereby creating a homogeneous system. In this situation, however, the solid polyolefin product has an irregular shape because the precipitation of the product from the homogeneous solution is unregulated [13, 14]. Accordingly, a solid support is required in order to use metallocene catalysts in heterogeneous commercial processes. For example, spherical silica gel has been used as a support material [15, 16].

With regard to activation of metallocene complex for olefin polymerization, a solid material other than the known homogeneous co-catalysts (MAO, borane, borate, or alkyl-aluminum) was proposed [17, 18, 19]. Mitsubishi Chemical Corporation and the group companies of Japan Polychem Corporation (JPC) pioneered the potential of clay minerals as an activator for the metallocene complex [17]. In 2002, Takahashi et al. carried out ethylene polymerization without the use of additional known homogeneous co-catalysts, using clay mineral supported metallocene catalysts. They concluded that some types of clay minerals behaved as co-catalysts and the acidity of clay minerals played an important role in the activation of metallocene catalysts [20]. Appropriate acid treatment of clay minerals enhanced the catalytic activity to a degree comparable to homogeneous co-catalysts [21].

In order to apply the metallocene based clay mineral catalysts for commercial use, the remaining issue to be

solved is the design of clay mineral particles to meet the process needs mentioned above. If the properties of clay mineral particles can be appropriately controlled, only one solid component will be necessary to fulfill the roles of both particle morphology control and metallocene activation [22]. Such a particle would be a brand-new Support-Activator. It is noted that catalysts consisting of a metallocene compound and a Support-Activator are cutting edge in the field of supported metallocene catalysts because an additional and chemically inert support, such as silica gel, is not required.

The objective of this work is to investigate the ability to control the particle morphology of montmorillonite in order to confirm the potential of clay minerals as a Support-Activator in the propylene polymerization catalyst system. Spray-dry granulation was employed. The granulation behavior influenced by the spray-dry conditions will be discussed from the viewpoint of the intrinsic nature of montmorillonite. Propylene polymerization, using metallocene catalysts supported on the clay mineral, was also performed to confirm the effects of granulation on polymer particle morphology.

## EXPERIMENTAL

### Materials

#### *Clay minerals*

Benclay SL and Purified Bentonite were purchased from Mizusawa Industrial Chemicals, Ltd. They are the same chemical substances: Benclay SL is a solid material and Purified Bentonite is water dispersion. Kunipia F was purchased from Kunimine Industry Co., Ltd. Synthetic mica (ME100) was obtained from Co-op Chemical Co., Ltd. Silica gel (SP9-261) was obtained from W. R. Grace and Co. –Conn.

#### *Metallocene compounds*

rac-(Dimethylsilylene)bis[1,1-{2-methyl-4-(4-chlorophenyl)-4-hydroazulenyl}]zirconium dichloride, which was developed by authors, was prepared according to the patent application [23]. The obtained product was characterized by  $^1H$ -NMR and used as a metallocene compound for the propylene polymerization catalysts.  $^1H$ -NMR spectra were recorded on a Varian Gemini-300 at 300 MHz.

#### *Other reagents*

Industrial grades of heptane and toluene were dried by molecular sieves (4A) and degassed by dry nitrogen bubbling before use.

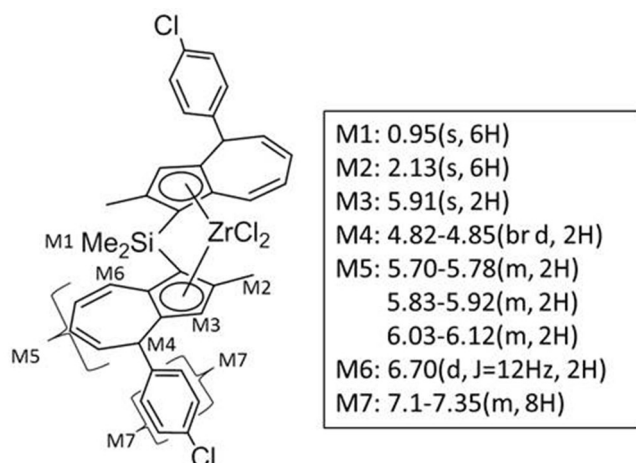


**Figure 1.** Structure of metallocene compound and characterization by  $^1\text{H-NMR}$ .

Alkyl aluminum reagents in hydrocarbon solvent were purchased from Tosoh Fine Chem Corporation and used without any further purification.

### Preparation of granulated clay minerals, supports and catalysts

#### *Spray-dry granulation of clay minerals*

Granulation was conducted by a spray-dry instrument (LT-8 of Ohkawara Kakohki Co., LTD.). Three liters of clay slurry were introduced into a 5 L metal vessel and homogenized by Ultra Turrax T25 of IKA Labortechnik for 10 min. Clay mineral granules were prepared in the following conditions; slurry feed rate (Q) : 0.6 or 1.5 kg/h, disk rotation speed (N) : 7000-30000 rpm, inlet air temperature: 130-230°C.

#### *Milling of montmorillonite*

Montmorillonite was milled by a counter jet mill (grinder: 100 AFG and size classifier: 50 ATP manufactured by Hosokawa Micron Corporation). Milling was performed under two different conditions. Preparation conditions for M-2 sample; air pressure: 0.6 MPa, powder feed rate: 0.5 kg/h, rotor speed: 1500 rpm. Preparation conditions for M-3 sample; air pressure: 0.6 MPa, powder feed rate: 0.7 kg/h and rotor speed: 11500 rpm.

#### *Preparation of supports for metallocene catalysts [24]*

To a separable four necked flask (2 L) equipped with a mechanical agitation unit, a water condenser, and a thermometer, 1130 mL of distilled water and 332 mL of conc. sulfuric acid were introduced. The mixture was heated to 90°C by oil bath, and 200 g of a clay mineral granulated by a spray-dryer was added. The mixture was stirred at 90°C for 3 h, and then cooled to room

temperature. The solid part was collected by filtration and washed with 2000 mL of cold distilled water 4 times. The washed cake was re-dispersed in 450 mL of water, and the resulting mixture was introduced into an aqueous solution (450 mL) of  $\text{Li}_2\text{SO}_4$  (226 g). The mixture was stirred at room temperature for 2 h. The solid part was collected by filtration and washed with 2000 ml of cold distilled water 4 times. Obtained cake of the clay mineral was dried in oven at 120°C overnight. By this drying, the wet cake became highly fluid powder. After removing an agglomerated portion in the dried powder, the remaining powder was dried under vacuum at 200°C for 2 h. The resulting clay mineral granules were stored as a support under dry  $\text{N}_2$  atmosphere.

#### *Preparation of supported metallocene catalysts*

All operations were carried out under dry  $\text{N}_2$  atmosphere using standard Schlenk techniques.

To a three necked flask (1 L) equipped with a mechanical agitation unit, 20.0 g of the support prepared as in the above section and 73 mL of dry heptane were introduced. To the resulting dispersion, heptane solution of tri-octyl-aluminum (50.0 mmol) was added and the mixture was stirred at 25°C for 1 h. After removal of the supernatant liquid by decantation, the solid material was washed twice with 900 mL of heptane. Then, total volume was adjusted to 100 ml by heptane addition and heptane solution of tri-isobutyl-aluminum (TiBA, 2.40 mmol) was added. After 5 min agitation, 600  $\mu\text{mol}$  of rac-(dimethylsilylene)bis[1,1-{2-methyl-4-(4-chlorophenyl)-4-hydroazulenyl}] zirconium dichloride, in 86 mL of heptane, was introduced. The mixture was stirred at room temperature for 1 h. Then, total volume of the resulting dispersion of the catalyst was adjusted to 500 mL by heptane addition, and the dispersion was transferred to a 1 L-autoclave with a mechanical stirrer and a temperature controller.

Pre-polymerization was carried out by feeding propylene continuously (constant rate 10 g / h) to the autoclave for 4 h at 40°C. After that propylene feed was stopped, the reaction was continued for 1 h. Then, the mixture was transferred to a 1 L flask, and the liquid phase was removed by cannula technique. Then, heptane solution of TiBA (12.0 mmol) was added to the dense slurry as a scavenger for catalyst poisons under mechanical agitation. Then the mixture was dried by vacuum evaporation at 40°C. The supported metallocene catalyst powder obtained was stored in dry  $\text{N}_2$  atmosphere.

## Characterization

### *Viscosity*

Clay mineral slurry was agitated for 3 h at 25°C, and viscosity was measured at 12 rpm by a B-type viscosity meter (LVDV-I viscometer of Brookfield engineering).

### *Chemical composition*

Al, Si, Mg, Fe and Na contents in clay mineral were determined by X-ray fluorescence (Rigaku ZNX-100e XRF spectrometer) by the calibration method.

### *Zeta electric potential*

Zeta potential of montmorillonite was measured by Zetasizer Nano ZS90 of Malvern. The slurry concentration of montmorillonite was 0.01 wt%.

### *Pore volume and surface area*

Nitrogen adsorption-desorption profiles at -196°C were obtained on a Quantachrome Autosorb 3B instrument. Prior to adsorption, samples were outgassed under vacuum (<1.3 Pa) at 200 °C for 2 h. Pore volume was determined by the BJH model.

### *XRD*

The XRD spectra of montmorillonite samples were obtained by a Rigaku diffractometer (RAD II B) using monochromatized CuK $\alpha$  radiation. The scan speed : 1°/min and scan range : 3° to 40° (2 $\theta$ ).

### *Particle size and particle size distribution*

The particle size and particle size distribution of clay mineral particles and granules were determined by a laser diffraction particle size analyzer (LA-920 of Horiba) in water or EtOH dispersion. Montmorillonite powder was introduced into the cell of the analyzer filled with solvent under agitation. The dispersion was sonicated for 5 min before measurements.

### *Determination of particle strength of granules*

Particle strength of spray-dried clay mineral granules was determined by a micro compression tester (MCTM-500 of Shimadzu). Strength was obtained as an average of more than 10 granule measurements.

### *SEM*

Particle morphology of spray-dried clay mineral granules was observed by a Real Surface View Microscope (VE-7800 of Keyence).

### *AFM*

Primary particles were observed by a nanoscale

hybrid microscope (VN-8000 of Keyence). Samples were prepared as follows; 20 mg/L aqueous dispersion of montmorillonite was dropped on mica substrate and dried at room temperature under air. Particle characteristics were determined by 100 particle measurements randomly chosen in the AFM view. Their perimeter, basal area, and thickness were determined by DFM mode. Aspect ratio was calculated by dividing an equivalent circle diameter based on basal area by thickness.

### *Acid titration*

The amount of surface hydroxyl groups of montmorillonite was determined by acid titration [25, 26]. Montmorillonite (1.0 g) was dispersed in 0.1 M aqueous solution of NaCl (100 mL), and high purity N<sub>2</sub> was bubbled into the slurry until its pH value became constant (about 2 h). pH of the slurry was continuously measured during titration with 0.1 M aqueous solution of HCl.

## Catalytic Tests

### *Co-polymerization of propylene and ethylene*

Polymerization was conducted in a 3 L autoclave with a mechanical stirrer and a temperature controller. To the autoclave, 750 g of propylene, 17.0 g of ethylene and 4.04 mmol of TiBA in heptane solution were introduced. To control molecular weight of polymer, 100 NmL of H<sub>2</sub> was introduced into the autoclave. The temperature was raised up to 70°C, and 20.0 mg of catalyst in 10 mL of heptane was introduced by argon pressure to start polymerization. After 1 h, polymerization was quenched by the addition of 5 mL of EtOH. The remaining monomer was purged and replaced by N<sub>2</sub>. The obtained propylene ethylene copolymer was recovered from the autoclave and dried for 1 h at 70°C.

### *Polymer characterization*

Melt flow rate (MFR) and powder bulk density (BD) were measured based on the industrial standard procedures described in JIS-6758[27] and ASTM D1895-69[28], respectively.

Particle size and its distribution were determined by CAMSIZER of Retsch Co., Ltd.

Fine content was determined by the following procedure: The whole polymer obtained by polymerization was poured onto a sieve (212  $\mu$ m opening) and shaken for 10 min. The weight percent of the fraction through the sieve was defined as fine content.

The comonomer incorporation in the copolymers and the stereoregularity of polymers were determined by  $^{13}\text{C}$  NMR [29, 30]. The copolymer solutions were prepared in o-dichlorobenzene as a solvent and benzene-d6 for an internal lock in a sample tube of 10 mm diameter. The  $^{13}\text{C}$  NMR spectra were recorded using a JEOL GSX-400 FT-NMR spectrometer. Spectra were taken with a  $90^\circ$  pulse angle, a pulse repeating of 15 s and 6000 scans at  $130^\circ\text{C}$ .

## RESULTS AND DISCUSSION

### Granulation of montmorillonite by a spray-dry method

The basic properties of clay minerals used in this study are shown in Table 1. The particle size shown is the median diameter determined by the laser diffraction/scattering method in water. Each material has a different primary particle size.

In order to address the practical limitations of the experimental instrument of spray-dry process, the upper limit of viscosity and a standard slurry concentration were determined using Purified Bentonite. The correlations between the slurry concentration and the viscosity of clay minerals and silica are shown in Figure 2.

The viscosity of Purified Bentonite showed a stronger dependence on concentration than that of silica. For instance, at a slurry concentration of 5 wt%, the viscosities of Purified Bentonite and silica gel were 5.9 and 0.8 mPa.s, respectively. As the concentration increased, the viscosity of the Purified Bentonite slurry increased more steeply than that of the silica slurry. When the concentration was higher than 6 wt%, the Purified Bentonite slurry no longer showed fluidity, although the silica slurry still showed a relatively

**Table 1.** Chemical composition and particle size of the clay-minerals used.

| Clay-mineral       | $\text{SiO}_2$ wt% | $\text{Al}_2\text{O}_3$ wt% | MgO wt% | $\text{Fe}_2\text{O}_3$ wt% | Na wt% | Dp50 ( $\text{H}_2\text{O}$ ) <sup>(a)</sup> $\mu\text{m}$ |
|--------------------|--------------------|-----------------------------|---------|-----------------------------|--------|--|
| Purified Bentonite | 72.0               | 16.8                        | 3.4     | 2.9                         | 2.6    | 0.6  |
| Kunipia-F          | 66.6               | 23.1                        | 3.5     | 2.1                         | 2.7    | 1.6  |
| ME-100             | 61.6               | <3.8                        | 28.2    | <0.7                        | 3.5    | 6.4  |

<sup>(a)</sup> Average particle size (median size) measured in water.

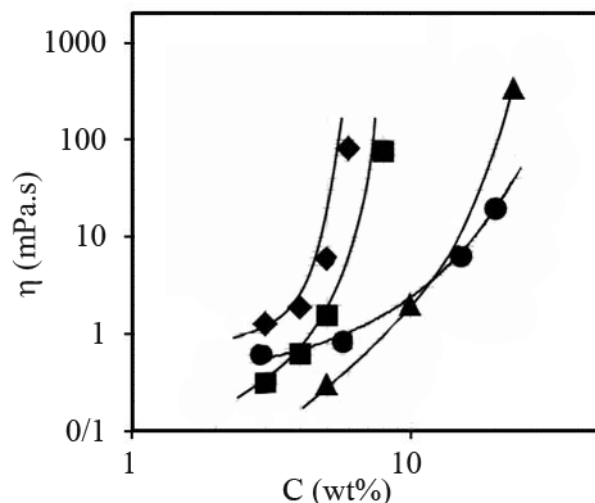


**Figure 2.** Correlations between viscosity and concentration of (♦) Purified Bentonite, (■) Kunipia-F, (▲) ME-100 and (●) silica.

lower viscosity. The spray-dry method is only applicable to Purified Bentonite within a narrow range of concentration. Therefore, a slurry concentration of 4 wt% was selected as the standard condition for the spray-dry granulation experiments. The results of spray-dry granulation are shown in Figure 3, where the particle size of the obtained granules ( $D_p$ ) (the median size measured in EtOH) is plotted against the disk rotation speed ( $N$ ). At a constant slurry feed rate ( $Q = 0.6$  kg/h),  $D_p$  is proportional to  $N^{-0.7}$  ( $7000$  rpm  $< N < 30000$  rpm) and adjustable in the range of 13 to  $38$   $\mu\text{m}$ .

A similar correlation is observed at a higher slurry feed rate ( $Q = 1.5$  kg/h) (note that the disk rotation speed is the same), however the granules obtained are

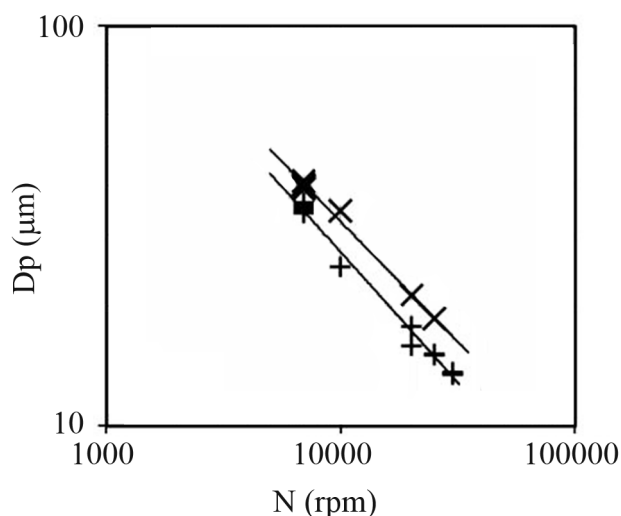


**Figure 3.** Correlations between particle size ( $D_p$ ) and disk rotation speed ( $N$ ). (×) slurry feed rate 1.5 kg/h, (+) slurry feed rate 0.6 kg/h.

**Table 2.** Preparation conditions and characteristics of granulated Purified Bentonite.

| Granule sample | Spray dry conditions <sup>a</sup> |                         | Characterization of granules |                                  |                          |
|----------------|-----------------------------------|-------------------------|------------------------------|----------------------------------|--------------------------|
|                | Q <sup>(b)</sup><br>kg/h          | N <sup>(c)</sup><br>rpm | Shape                        | Dp50<br>(EtOH) <sup>(d)</sup> μm | St <sup>(e)</sup><br>MPa |
| S-1            | 0.6                               | 7000                    | Irregular                    | 35                               | 15                       |
| S-2            | 0.6                               | 15000                   | Spherical                    | 26                               | 17                       |
| S-3            | 0.6                               | 20000                   | Spherical                    | 16                               | 17                       |
| S-4            | 1.5                               | 7000                    | Irregular                    | 39                               | 14                       |
| S-5            | 1.5                               | 20000                   | Spherical                    | 21                               | 16                       |

<sup>(a)</sup> Concentration of slurry = 5wt%. <sup>(b)</sup> Slurry feed rate. <sup>(c)</sup> Disk rotation speed. <sup>(d)</sup> Average particle size (median size) measured in EtOH. <sup>(e)</sup> Particle strength.

larger (18 to 41 μm). The correlation between Dp and Q, with constant N, was also investigated using the data set of Dp and Q at the same N value, as shown in Figure 3. In this case, Dp is proportional to  $Q^{0.2}$ .

Overall, the particle size was controlled within the range of 12 μm to 40 μm when 4 wt% of Purified Bentonite was used. It was also observed that large particles were formed at lower disk rotation speeds (N (rpm)) or higher slurry feed rates (Q (kg/h)). Therefore, the size of the slurry droplets is influenced by N and Q. The spray-drying of Purified Bentonite follows general granulation rules [31]. Consequently, we found that the granule size of Purified Bentonite could be controlled by the slurry feed rate and the disk rotation speed during the spray-dry method.

Examples of SEM images of typical granule shapes are shown in the upper part of Figure 4, spherical (S-3 (right)) and irregular (S-1 (left)). Spray-drying conditions and the properties of produced granules are summarized in the upper part of Table 2. Smaller granules, with a median size in EtOH of 16 to 26 μm, have a spherical shape (Figure 4) (S-3)), whereas, larger granules, with a median size larger than 30 μm, have an irregular shape (Figure 4) (S-1)).

Consequently, granule shape was strongly influenced by spray-dry conditions. Spherical granules were obtained only in the conditions for smaller granules, and vice versa.

A plausible drying mechanism is shown in Figure 5. Slurry droplets pass through a stage during which a type of “core-shell” structure is formed. Throughout this stage, the surface (shell) is dry but the internal core remains wet. In the case of smaller slurry

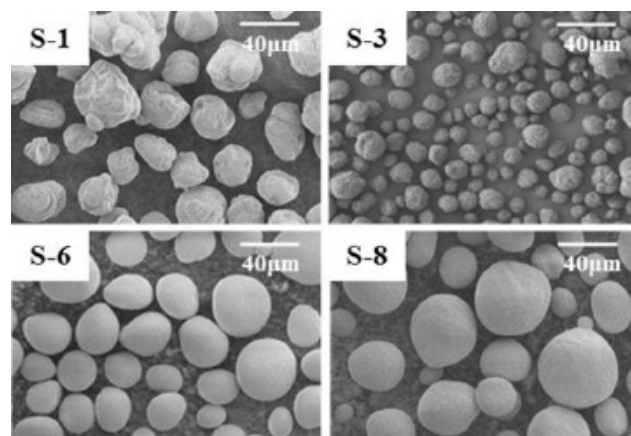


**Figure 4.** SEM images of spray-dried particles using Purified Bentonite and milled Benclay SL. Upper part: Granulated particles of Purified Bentonite, Left: (S-1) Larger but irregular, Right: (S-3) Smaller and spherical, Lower part: Granulated particles of milled Benclay SL as larger and spherical examples, Left: (S-6) Granulated M-2, Right: (S-8) Granulated M-3.

droplets, water vaporization is completed rapidly because only a small quantity of water is contained inside. Drying occurs uniformly, resulting in spherical particles. In contrast, in the case of larger droplets, water remains within the core even after formation of the outer shell. Since the temperature is higher than the boiling point of water, water vaporizes inside the particle. This vaporization induces an increase in the internal pressure of the particle. The formed shell cannot withstand the increase in pressure and fractures due to spouting vapor, thus producing irregular shape granules [32].

To avoid such phenomenon, slower vaporization or a higher slurry concentration of droplets seems to be effective for the production of larger spherical particles. Meanwhile, some of the irregular shaped larger particles have an agglomerated structure, as shown in Figure 4 (S-1). These agglomerated granules are likely formed by the coagulation of wet particles before drying is completed. To avoid agglomeration,

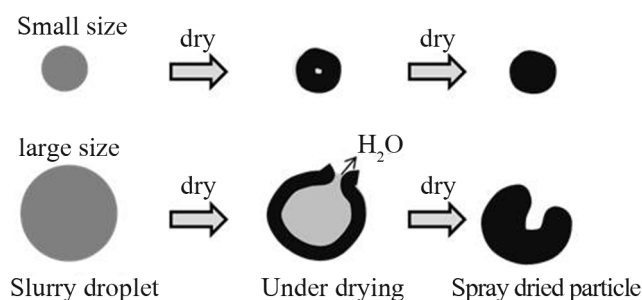


**Figure 5.** A plausible drying mechanism in spray drying.

evaporation of water from droplets should be completed rapidly. For this purpose, a highly concentrated slurry is optimal for spray-drying because a lower quantity of water is required to be removed.

The particle strength of the granulated Purified Bentonite did not depend on the conditions of spray-drying, as shown in Table 2.

Consequently, we succeeded in preparing spherical granules of montmorillonite by the spray-dry method with sizes ranging from 10 to 30  $\mu\text{m}$ . However, the preparation of larger spherical granules ( $>30 \mu\text{m}$ ) by this method was unsuccessful because the highly concentrated slurry that was required was difficult to spray due to its high viscosity. The higher slurry concentration is, the drastically higher the viscosity of the slurry becomes, which is not a specific behavior in the current system but a typical one for montmorillonite because of its swelling character in water dispersion. This problem must be overcome because larger spherical granules are required for the catalyst system of propylene polymerization in gas phase reactors.

#### **Investigation of methods to reduce viscosity in aqueous montmorillonite slurries**

In order to obtain larger, spherical granules by the spray-dry method, a highly concentrated and less viscous slurry of montmorillonite is required. To overcome this difficulty, we tried to reduce particle-water interactions by modifying particle-particle interactions. We examined the following three approaches:

- Changing the electrochemical properties of the clay mineral surface.
- Changing the electric density in the solvent by the addition of electrolytes.
- Changing the morphology of montmorillonite.

#### *Reduction of the interaction among particles and water by changing electrochemical properties of the clay mineral surface*

In order to examine the effect of clay mineral surface properties on slurry viscosity, synthetic mica (ME100) was used for comparison. ME100 consists of  $\text{MgO}$  and  $\text{SiO}_2$ . All of the OH groups on the surface of the Si species have been replaced by F atoms. Therefore, the surface properties must be quite different from that of montmorillonite, and must be good reference to know the relationship of slurry concentration and surface

chemical properties.

In Figure 2, the relationships between the aqueous slurry concentration and the viscosity of Purified Bentonite, Kunipia-F, and ME100 are shown. The ME100 slurry shows a lower viscosity than the other materials at all concentrations. Clearly, the use of F atoms to change the surface properties is an effective approach to reducing slurry viscosity.

We then examined spray-dry granulation with a high concentration (18 wt%) slurry of ME100 in water, in which the slurry viscosity was still under the upper limit of the instrument (10 mPa.s). Spherical granules having the median diameter  $D_p = 59 \mu\text{m}$  were obtained at a disk rotation speed of 15000 rpm. As expected, the high slurry concentration gives larger and spherical granules. However, the strength of the obtained particles is quite low (3 MPa) and it is too weak to use as a support for propylene polymerization catalysts.

This low particle strength might be caused by two factors. First, granulated ME100 might have fewer contact points because its particle size in water is very large compared with those of the montmorillonite that were previously used. Secondly, it was thought that the peel strength of each contact point was weak because there are no OH groups on the surface of ME100.

These model experiments using ME100 strongly suggest that it is important to use less viscous and highly concentrated slurry for spray-dry granulation in order to obtain larger spherical granules.

#### *Reduction of the interaction among particles and water by changing the electric density of the solvent through the addition of an electrolyte*

As described above, water is commonly used as the dispersion medium for montmorillonite. Interestingly, it is known that the addition of an electrolyte to a water dispersion of montmorillonite influences the viscosity of the slurry [33, 34]. This behavior is explained by agglomeration and swelling of montmorillonite. Therefore, we expected that the viscosity of the montmorillonite slurry in water containing an electrolyte might show a lower viscosity than that of the slurry in pure water. We used NaCl as the electrolyte in this study.

Montmorillonite slurry samples (5 wt%) were prepared using different NaCl contents, 0.4, 0.8, and 1.2 mM. The slurry viscosities of these samples were 6.5, 6.6 and 7.1 mPa.s, respectively. These values

were higher than that of the sample prepared without an electrolyte (5.9 mPa.s). Indeed, the properties of montmorillonite slurry were influenced by NaCl in water, but unfortunately, the results were undesirable.

*Reduction of the interaction between particles and water by changing the morphology of montmorillonite*

It was previously reported that larger montmorillonite particles collected by elutriation showed lower viscosity in water [35, 36]. We expected that specific montmorillonite whose natural particle size was larger might interact with each other more weakly in water, thus showing lower slurry viscosity.

The correlation between concentration and viscosity was measured using Kunipia F because its particle size in water is larger than that of Purified Bentonite (0.6  $\mu\text{m}$ ), as shown in Table 1. Indeed, the viscosity of Kunipia F is slightly lower than that of Purified Bentonite. However, the viscosity increases drastically as the concentration increases (Figure 2), in a similar fashion to that of Purified Bentonite. In addition, the degree of the viscosity decrease is equal to only a 1-2 wt% increase of concentration, and not large enough to obtain larger spherical granules. We gave up this approach for the production of larger spherical granules.

Next, we attempted milling of montmorillonite to decrease the aspect ratio. Because Suzuki, et al. reported that slurry of montmorillonite with a lower aspect ratio showed lower viscosity [37], Benclay SL was milled by a counter jet mill (JM) consisting of a jet mill and a rotor-type size fractionator. By modifying the operation conditions of these two parts, the degree of milling can be controlled. In this work, two milled samples were prepared.

In Figure 6, the correlation between slurry concentration and viscosity is shown. M-1 is the un-milled reference. As the concentration of slurry in water increases, the viscosity also increases, even in the case of milled materials, M-2 and M-3. However, the slurry viscosity of the milled materials at higher slurry concentrations (>5 wt%) is lower than that of the un-milled material, M-1. Slurry viscosity of M-3 is lower than that of M-2 at all concentrations [38].

Based on these results, we prepared two slurry samples containing 10 wt% of M-2 and 12 wt% of M-3, having higher concentrations than that of the un-milled sample (4 wt%). Larger and smaller granules were prepared at rotation speeds of 7000 and 20000

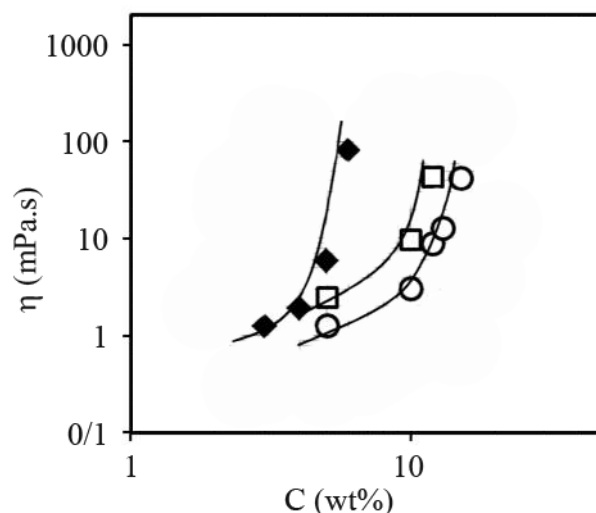


**Figure 6.** Correlations between viscosity and concentration of (◆) Purified Bentonite, (□) M-2; milled Benclay SL, (○) M-3; milled Benclay SL.

rpm, respectively.

The results are shown in Table 3. All granule samples (S-6 – S-9) are spherical, as shown in the lower part of Figure 4. S-6 and S-8 have good spherical shapes and very smooth surfaces, compared with the un-milled montmorillonite. However, particle strength (St) is in the range of 10 to 17 MPa, which is slightly lower than that of the un-milled material. Milling montmorillonite is therefore an effective method to produce spherical granules up to a size of 50  $\mu\text{m}$  with moderate strength.

In order to understand why milling reduced the slurry viscosity of montmorillonite, the physical properties were investigated, as shown in Table 4. Both the surface area and pore volume of montmorillonite increase as a result of milling. The particle size of M-1 dispersed in EtOH is 17.8  $\mu\text{m}$ , whereas the milled samples of M-2 and M-3 dispersed in EtOH have particle sizes of 3.7 and 2.6  $\mu\text{m}$ , respectively. The particle size decreases as a result of milling. According to the literature [39], clay minerals do not swell or disperse in EtOH. Therefore, the particle size in EtOH corresponds to the inherent size of the clay minerals, that is, the primary particle size.

On the other hand, because montmorillonite swells and disperses in water, the particle size measured in water is influenced by these behaviors [39]. As shown in Table 4, the particle sizes of M-2 and M-3 in water are the same, 0.9  $\mu\text{m}$ , but are larger than that of M-1 (0.6  $\mu\text{m}$ ). Because, inherently, M-2 and M-3 are smaller than the original M-1, as clearly shown above, the increase of their particle size in water

**Table 3.** Preparation conditions and characteristics of granulated Benclay SL.

| Granule sample | Milled sample | Spray dry conditions <sup>(a)</sup> |                         | Characterization of granules |                                 |                          |
|----------------|---------------|-------------------------------------|-------------------------|------------------------------|---------------------------------|--------------------------|
|                |               | C <sup>(b)</sup><br>wt%             | N <sup>(c)</sup><br>rpm | Shape                        | Dp50(EtOH) <sup>(d)</sup><br>µm | St <sup>(e)</sup><br>MPa |
| S-6            | M-2           | 10                                  | 7000                    | Spherical                    | 48                              | 10                       |
| S-7            | M-2           | 10                                  | 20000                   | Spherical                    | 19                              | 17                       |
| S-8            | M-3           | 12                                  | 7000                    | Spherical                    | 49                              | 12                       |
| S-9            | M-3           | 12                                  | 20000                   | Spherical                    | 22                              | 16                       |

<sup>(a)</sup> Slurry feed rate = 1.0 kg/h, <sup>(b)</sup> Concentration of Slurry, <sup>(c)</sup> Disk rotation speed, <sup>(d)</sup> Average particle size (median size) measured in EtOH, <sup>(e)</sup> Particle strength.

strongly suggests that milling changes their dispersion properties in water. Consequently, milling changes not only the morphology, but also the surface chemical properties, which contribute to the reduction in slurry viscosity.

In this section, various approaches were taken to obtain the desired aqueous slurry of montmorillonite with low viscosity, even with a high concentration. We found that milling montmorillonite was the only way to meet these objectives.

#### *Investigation of the milling effect on clay properties*

In order to confirm the swelling properties of milled montmorillonite in water, further evaluations of both morphology and chemical properties were performed. Analyses of the morphology changes caused by milling were conducted using XRD and AFM measurements. In Figure 7, the XRD charts of M-1, M-2 and M-3, which were pretreated with ethylene glycol, are shown.

Treatment with ethylene glycol seemed to cause intercalation of glycol molecules into the interlayer of montmorillonite [40]. The strong signal at  $2\theta = 7^\circ$  was assigned as d(001) of basal reflections of the montmorillonite structure. By milling, only the intensity of this signal was weakened in the charts

of M-2 and M-3, and no change was observed in the intensities of other signals, including the opal signal. Accordingly, cleavage was the major structural change induced by the milling, resulting in a reduction of the number of layers in montmorillonite primary particle.

Figure 7 shows AFM photos of M-1, M-2 and M-3. The perimeters, basal areas, and aspect ratios of each were determined by AFM [41]. And the results are summarized in Table 4. The perimeters, basal areas, and aspect ratios of M-2 and M-3 were slightly smaller (within 10 %) than the values of the un-milled sample (M-1).

Based on XRD and AFM results, it was found that milling induced layer cleavage and tiny edge chipping in montmorillonite particles. However, the reduction in aspect ratio of the basal plane caused by chipping is within 10 %. Such small changes could not be considered as the cause of the lower slurry viscosity in milled montmorillonite dispersions [37]. XRD and AFM clearly indicate that the change in physical structure of montmorillonite is not the reason why the viscosity of the slurry was reduced by milling (shown in Figure 6). However, the change in chemical structure of the montmorillonite surface that is induced by milling is extremely important. To examine the change in the chemical properties induced by milling,

**Table 4.** Physical properties of Benclay SL samples milled by JM.

| Sample | Mill | BET                      |                         | Particle Size                   |   | AFM             |                                      |                 |
|--------|------|--------------------------|-------------------------|---------------------------------|---|-----------------|--------------------------------------|-----------------|
|        |      | PV<br>cm <sup>3</sup> /g | SA<br>m <sup>2</sup> /g | Dp50(EtOH) <sup>(a)</sup><br>µm | Dp50(H <sub>2</sub> O) <sup>(b)</sup><br>µm | Perimeter<br>µm | BA <sup>(c)</sup><br>µm <sup>2</sup> | Aspect<br>ratio |
| M-1    | No   | 0.215                    | 74                      | 17.8                            | 0.6   | 0.578           | 2.17×10 <sup>-2</sup>                | 222.4           |
| M-2    | Yes  | 0.406                    | 97                      | 3.7                             | 0.9   | 0.571           | 2.10×10 <sup>-2</sup>                | 216.4           |
| M-3    | Yes  | 0.428                    | 90                      | 2.6                             | 0.9   | 0.544           | 1.98×10 <sup>-2</sup>                | 197.5           |

<sup>(a)</sup> Average particle size (median size) measured in EtOH, <sup>(b)</sup> Average particle size (median size) measured in water, <sup>(c)</sup> Basal area.

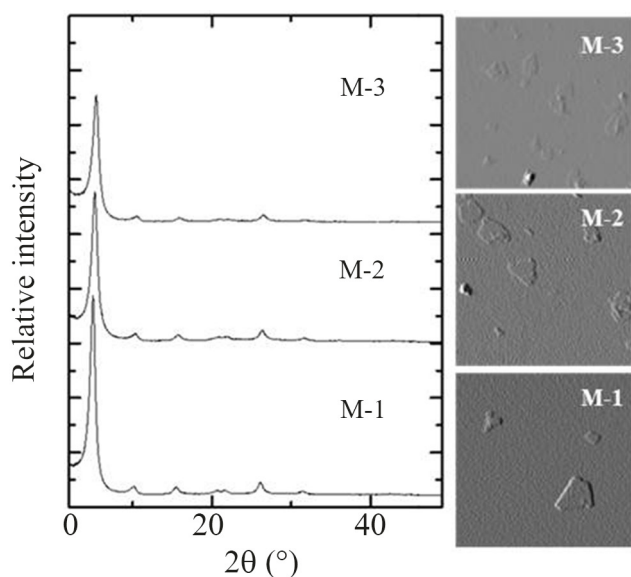


**Figure 7.** XRD profile and AFM images of the Purified Bentonite milled by JM.

the amount of surface OH groups of milled and unmilled montmorillonite materials was measured by acid titration, as described in the Experimental section.

In Figure 8, the results of the titration of unmilled (M-1) and milled (M-3) montmorillonite are shown. In the region of  $\text{pH} > 7$ , the titration curves of M-1 and M-3 are the same. At  $\text{pH} = 7$ , both the curves begin to separate from each other and continue to separate in the region of  $\text{pH} < 7$ , indicating that M-3 has more surface OH groups than M-1. The surface OH groups of montmorillonite are from silanol (SiOH) and aluminol (AlOH), which are located at the edge face.

The titration curves depend on the dissociation rate constants [42]. The amount of titrate is proportional to the quantity of surface OH groups. Milled (M-3) montmorillonite has more surface OH groups than M-1, which shows that new edges are formed by milling.

To clarify the effect of milling on the properties of montmorillonite, zeta electric potentials were measured. An aggregated particle size was calculated and plotted in Figure 8 as a function of the slurry pH. The aggregated particle size of unmilled M-1 is always within the narrow range of 0.6 to 1.1  $\mu\text{m}$ , irrespective of the pH value. In contrast, in the cases of M-2 and M-3, the aggregated particle size changed according to the pH value. In the region of low pH ( $\text{pH} < 4$ ), the aggregated particle size was larger, and overall, M-3 showed larger particle sizes than M-2. In the region of  $\text{pH} > 6$ , the aggregated particle size became smaller (2.5–4.0  $\mu\text{m}$ ).

As described above, milling induces the aggregation of montmorillonite in water. This aggregation is most likely the reason why the slurry viscosity of milled materials is lower than that of unmilled materials.

The image of structural change in montmorillonite by milling is shown in Figure 9. Besides a small change in particle size and aspect ratio, the number of surface OH groups at the edges significantly increases by chipping and wearing of edges through the milling operation. Unmilled montmorillonite is highly dispersed in water, whereas milled montmorillonite

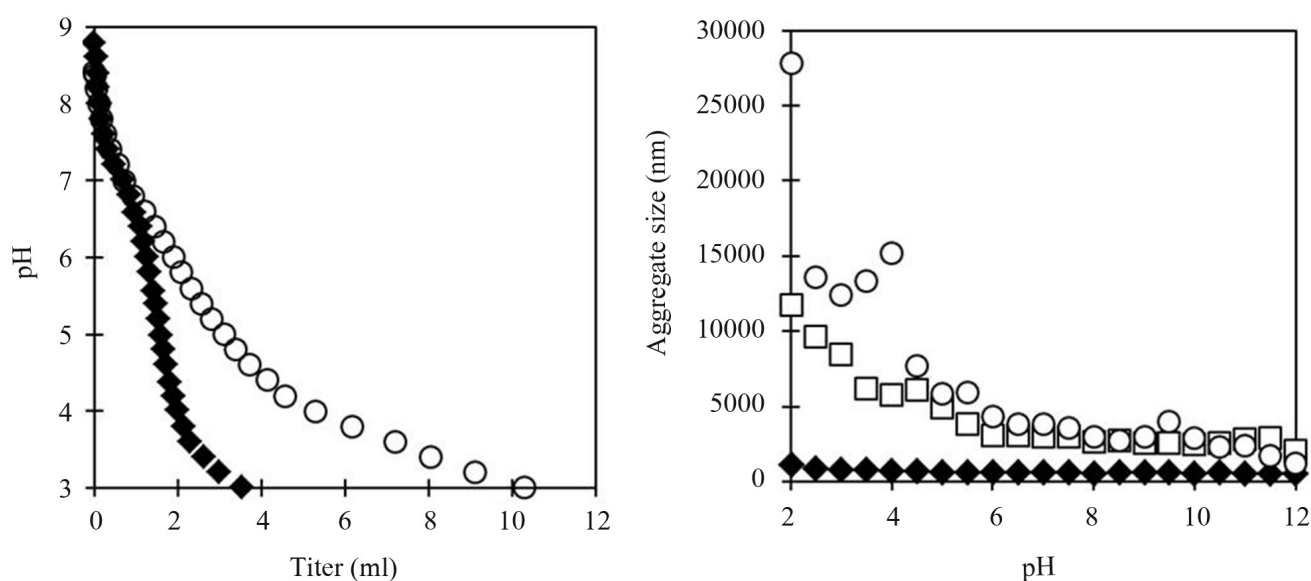


**Figure 8.** Evaluation results of Zeta electric potential measurement. Left: Slurry pH changes by acid titration, Right: Correlations between aggregate size and pH, (♦) Purified Bentonite, (□) M-2: milled Benclay SL, (○) M-3: milled Benclay SL.

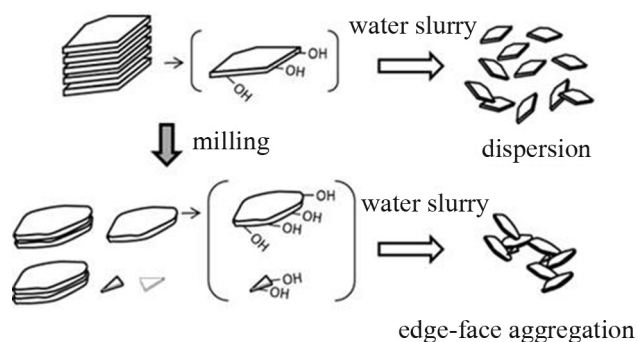


**Figure 9.** Schematic aggregation mechanism of montmorillonite by milling.

aggregates in water, since a large number of OH groups induce strong electrostatic interactions between the edge and basal planes [34]. As a result, milling of montmorillonite decreases the slurry viscosity.

### Propylene polymerizations with catalysts prepared with granulated clay solids

Catalysts were prepared using various types of granulated montmorillonite as support, which were subsequently used for the polymerization of propylene. All results are summarized in Table 5. Optical microscopy photos of two typical polymer powders are shown in Figure 10.

Catalysts prepared using S-1 and S-3 (Figure 4) as typical supports composed of un-milled montmorillonite, were used for polymerization (run No P-1 and P-2, respectively in Table 4). The morphologies of the obtained polymer powders clearly reflect the shape of the supports. For instance, S-1 has an irregular shape and the corresponding polymer powder has an irregular surface, as well as a lower bulk density. On the other hand, the powder obtained in run No P-2, in which spherical S-3 was used, has a nicely spherical shape and a higher bulk density. Regarding

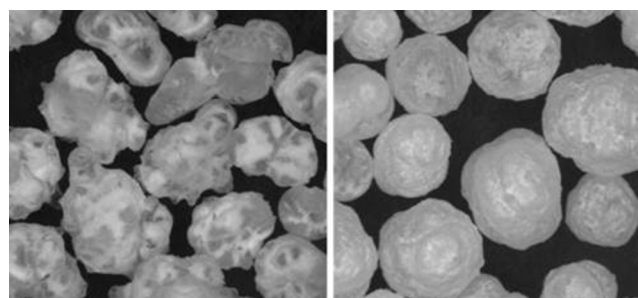


**Figure 10.** Optical microscope images of PP powder. Left: P-1 powder obtained from S-1 support, Right: P-3 powder obtained from S-6 support.

fine content of the product, the polymer powder produced from the irregular shaped catalyst had higher fine content. The more fines may be generated by friction caused between irregular particles rubbing against each other during polymerization. Therefore, it is very important for propylene polymerization catalysts to have a spherical shape.

Experiments P-3 to P-5 were performed using catalysts prepared with granulated supports of milled montmorillonite. All products showed excellent powder morphologies, which were independent of the size of the granulated support particle. As in the case of conventional heterogeneous Ziegler-Natta catalysts, polymer growth using metallocene catalysts supported on morphology-controlled montmorillonite basically follows the replica rule.

Regarding the macroscopic particle morphology control, however, Table 5 and Figure 10 clearly indicate that the montmorillonite granules by spray-drying have the spherical shape even after acid treatment. Therefore, the spray-dry granulation of the montmorillonite is recognized as the excellent method for the metallocene supported olefin polymerization catalysts, which is commercially applicable.

**Table 5.** Results of propylene polymerization using metallocene catalysts.<sup>(a)</sup>

| Run | Granule sample | Mill | Powder shape | Activity g-PP/g-cat | Mw ×10 <sup>4</sup> | Mw/Mn | [mm] %  | [C <sub>2</sub> ] <sup>(b)</sup> wt% | BD <sup>(c)</sup> g/cm <sup>3</sup> | Fine ratio wt% |
|-----|----------------|------|--------------|---------------------|---------------------|-------|---------|--------------------------------------|-------------------------------------|----------------|
| P-1 | S-1            | No   | Irregular    | 27000               | 28.4                | 2.45  | 98.0    | 2.0                                  | 0.36                                | 0.33           |
| P-2 | S-3            | No   | Spherical    | 34000               | 32.9                | 2.37  | No data | 1.9                                  | 0.46                                | 0.01           |
| P-3 | S-6            | Yes  | Spherical    | 26000               | 32.8                | 2.42  | No data | 1.9                                  | 0.47                                | 0.12           |
| P-4 | S-7            | Yes  | Spherical    | 28000               | 29.9                | 2.43  | No data | 1.9                                  | 0.49                                | 0.03           |
| P-5 | S-8            | Yes  | Spherical    | 24000               | 27.3                | 2.34  | No data | 1.9                                  | 0.44                                | 0.10           |

<sup>(a)</sup> Propylene and ethylene copolymerization, <sup>(b)</sup> [C<sub>2</sub>] is ethylene content in propylene and ethylene copolymer, <sup>(c)</sup> Bulk density.

## CONCLUSION

Control of particle morphology using the spray-dry method was investigated in order to use montmorillonite as a support and co-catalyst for propylene polymerization catalysts. We successfully demonstrated that the spray-dry method, combined with milling, was effective and useful in making larger, spherical, and strong supports. The investigated granulation behavior and milling effects are summarized as follows:

1. Only smaller spherical granules ( $D_p = 10$  to  $30 \mu\text{m}$  in EtOH) were successfully prepared using a typical spray-dry method. A highly concentrated slurry was required for the preparation of large ( $>30 \mu\text{m}$ ) and spherical granules, which was not applicable to the instrument because of the upper limit of viscosity in spray-dryer operations.
2. A slurry of milled montmorillonite in water showed lower viscosity than that of un-milled particles. The milling of montmorillonite was effective in producing spherical granules, up to  $50 \mu\text{m}$  in size, with moderate strength.
3. We examined the mechanism by which milling caused a decrease in the slurry viscosity. The surface OH groups of the montmorillonite seem to play a key role in the interaction between the edge and basal planes. This interaction accelerates agglomeration of milled montmorillonite, which is considered to induce a lower slurry viscosity.
4. Propylene polymerization catalysts prepared from the granulated montmorillonite particles were investigated. The montmorillonite granules, prepared by the combination of milling and spray-drying, were excellent support materials for the polymerization catalyst.

## ACKNOWLEDGEMENTS

We express our gratitude to Professor Shoji Hara in Hokkaido University for his kind and helpful comments and advice on our work.

We gratefully acknowledge Hokkaido University and Mizusawa Industrial Chemicals, Ltd. for their

kind supports. We express our acknowledgement to Mitsubishi Chemical Corporation and Japan Polychem Corporation for the support and the approval of publication. And many thanks go to Inorganic Analysis Group, Analytical Technology Laboratory of Mitsubishi Chemical Corporation for carrying out analytical experiments and helpful discussions.

## REFERENCES

1. Floyd S, Heiskane T, Taylor TW, Mann GE, Ray WH (1987) Polymerization of olefins through heterogeneous catalysis. VI. Effect of particle heat and mass transfer on polymerization behavior and polymer properties. *J Appl Polym Sci* 33: 1021-1065
2. Hutchinson RA, Chen CM, Ray WH (1992) Polymerization of olefins through heterogeneous catalysis X: Modeling of particle growth and morphology. *J Appl Polym Sci* 44: 1389-1414
3. Kakugo M, Sadatoshi H, Sakai J, Yokoyama M (1989) Growth of polypropylene particles in heterogeneous Ziegler-Natta polymerization. *Macromolecules* 22: 3172-3177
4. Galli P, Haylock JC (1991) Continuing initiator system developments provide a new horizon for polyolefin quality and properties. *Prog Polym Sci* 16: 443-462
5. Edward P, Moore JR (1996) Catalysts and polymerizations. In: *Polypropylene handbook*, Hanser/Grandner publications, Inc., Cincinnati, 11-45
6. Bernard A, Fiasse P (1990) Catalytic olefin polymerization. Kodansha Ltd., 405-423
7. Pasquon I, Giannini U (1984) *Catalysis science and technology* Vol.6, Chapter 2, Springer Verlag, New York, Tokyo
8. Ewen JA, Johnes RL, Razavi A, Ferrara JD (1988) Syndiospecific propylene polymerizations with Group IVB metallocenes. *J Am Chem Soc* 110: 6255-6256
9. Sugano T, Tayano T, Uchino H, Ioku A, Iwama N, Endo J, Osano Y (1999) Novel metallocene catalyst for propylene polymerization. In: SPO99. Houston, USA
10. Cai Z, Nakayama Y, Shiono T (2006) Living random copolymerization of propylene and norbornene with *ansa*-Fluorenyl amido

- dimethyl titanium complex: Synthesis of novel syndiotactic polypropylene-b-poly (propylene-ran-norbornene). *Macromolecules* 39: 2031-2033
11. Hlatky GG, Turner HW, Eckman RR (1989) Ionic, base-free zirconocene catalysts for ethylene polymerization. *J Am Chem Soc* 111: 2728-2729
  12. Yang X, Stern CL, Marks TJ (1991) Cation-like homogeneous olefin polymerization catalysts based upon zirconocene alkyls and tris(pentafluorophenyl) borane. *J Am Chem Soc* 113: 3623-3625
  13. Kioka M, Toyota A, Kashiwa N, Tsutsui T (2000 May 16) Catalyst for polymerizing alpha-olefins and process for polymerization. US Patent 6,063,726
  14. Ewen JA, Welborn HCJR (1985 July 23) Process and catalyst for producing polyethylene having a broad molecular weight distribution. US Patent 4,530,914
  15. Chien JCW, He D (1991) Olefin copolymerization with metallocene catalysts. III. Supported metallocene/methylaluminoxane catalyst for olefin copolymerization. *J Polym Sci A: Polym Chem* 29: 1603-1607
  16. Kaminsky W (1995) How to reduce the ratio MAO/metallocene. *Macromol Symp* 97: 79-89
  17. Suga Y, Maruyama Y, Isobe E, Suzuki T, Shimizu F (1994 May 3) Catalyst for polymerizing an olefin and method for producing an olefin polymer. US Patent 5,308,811
  18. Weiss K, Wirth-Pfeifer C, Hoffmann M, Botzenhardt S, Lang H, Bruning K, Meichel E (2002) Polymerization of ethylene or propylene with heterogeneous metallocene catalysts on the clay. *J Mol Catal A: Chem* 182-183: 143-149
  19. Sano T, Niimi T, Miyazaki T, Tsubaki S, Oumi Y, Uozumi T (2001) Effective activation of metallocene catalyst with AIMCM-41 in propylene polymerization. *Catal Lett* 71: 105-110
  20. Takahashi T, Nakano H, Uchino H, Tayano T (2002) Study of the clay mineral "support-activator" in metallocene catalyst. *Polym Prepr* 43: 1259
  21. Suga Y, Isobe E, Suzuki T, Fujioka K, Ishihama Y, Sagae T, Go S, Uehara Y (1999) Novel clay mineral-supported metallocene catalysts for olefin polymerization. In: *MetCon'99 polymers in transition*, Houston, USA
  22. Tayano T, Sugawara M (2000) Advanced metallocene technology for propylene random copolymer. In: *MetCon'2000 Polymers in transition*, Houston, USA
  23. Sugano T, Iwama N, Isobe E, Suzuki T, Maruyama Y, Hayakawa A, Shoda H, Kashimoto M, Kato T, Aoshima T, Nishimura A, Suga Y, Sieber S (1999 May 20) Transition metal compounds. US Patent Appl. No. 09/315,131
  24. Uchino H, Itoh M, Ishihama Y, Nakano M (2010 Oct 6) Propylene-based polymer, production method therefor, composition using the same, and application thereof. JP Patent 4,558,066
  25. Fukushi K, Suzuki M (2004) Surface complexation modeling of the acid/base chemistry of natural allophane. *J Clay Sci Soc* 43: 180-185
  26. Rozalen M, Brady PV, Huertas FJ (2009) Surface chemistry of K-montmorillonite: Ionic strength, temperature dependence and dissolution kinetics. *J Colloid Interf Sci* 333: 474-484
  27. Japan Industrial Standard (2010) Plastics-polypropylene (PP) molding and extrusion materials- Part 2: Preparation of test specimens and determination of properties. JIS K6921-2
  28. American society for testing and materials (2010) Standard test methods for apparent density, bulk factor, and pourability of plastic materials. ASTM D1895-96
  29. Tsutsui T, Ishimaru N, Mizuno A, Toyota A., Kashiwa N (1989) Propylene homo- and copolymerization with ethylene using an ethylenebis(1-indenyl)zirconium dichloride and methylaluminoxane catalyst system. *Polymer* 30: 1350-1356
  30. Ray GJ, Johnson PE, Knox JR, (1977) Carbon-13 nuclear magnetic resonance determination of monomer composition and sequence distribution in ethylene-propylene copolymers prepared with a stereoregular catalyst system. *Macromolecules* 10: 773-778
  31. Fraser RP, Dombrowski N, Routley JH (1963) The atomization of a liquid sheet by an impinging air stream. *Chem Eng Sci* 18: 339-353
  32. Charlesworth DH, Marshall WRJR (1969) Evaporation from drops containing dissolved solids. *AIChE J* 6: 9-23
  33. Abend S, Lagaly G (2000) Sol-gel transition of sodium montmorillonite dispersions. *Applied Clay Science* 16: 201-227
  34. Armando GR, Torre L, Garcia-Serrano LA, Aguilar-

- Elguezbal A (2004) Effect of dialysis treatment on the aggregation state of montmorillonite clay. *J Colloid Interf Sci* 274: 550-554
35. Allan K (1958) The flocculation of sodium montmorillonite by electrolytes. *J Colloid Sci* 13: 51-60
36. Brandenburg U, Lagaly G (1988) Rheological properties of sodium montmorillonite dispersions. *Appl Clay Sci* 3: 263-279
37. Suzuki K, Sato T, Yoneda T (2012) Factors affecting to the viscosity of montmorillonite/water suspension 2. Relationship between aspect ratio of montmorillonite particles and viscosity of aqueous suspension. *J Clay Sci Soc* 50: 162-174
38. Sagae T, Atsumi T, Uchino H, Murata M, Tayano T, Satou T (2014) Morphology control of clay-mineral particles as supports for metallocene catalysts in propylene polymerization. In: 58<sup>th</sup> Clay Science Forum. Fukushima, Japan
39. Watanabe T (2009) Particle size distribution measurement. In: *Handbook of clays and clay minerals*, 3<sup>rd</sup> ed., Gihodobooks, Tokyo, 395-401
40. Watanabe T (2009) XRD measurement. In: *Handbook of clays and clay minerals*, 3<sup>rd</sup> ed., Gihodobooks, Tokyo, 373-376
41. Yokoyama S, Kuroda M, Sato T (2005) Atomic force microscopy study of montmorillonite dissolution under highly alkaline condition. *Clays Clay Miner* 53: 147-154
42. Rozalen M, Brady PV, Huertas FJ (2009) Surface chemistry of K-montmorillonite: Ionic strength, temperature dependence and dissolution kinetics. *J Colloid Interf Sci* 333: 474-484